Journal of Nanoscience and Nanoengineering
Vol. 1, No. 4, 2015, pp. 206-213
http://www.aiscience.org/journal/jnn

Nano-Scale Effect in Adhesive Friction of Sliding Rough Surfaces

Prasanta Sahoo*

Department of Mechanical Engineering, Jadavpur University, Kolkata, India

Abstract

Study of contact and friction at multiple length scales is necessary for the effective design and analysis of surfaces in sliding micro- and nano-electromechanical systems (MEMS/NEMS). As loading forces decrease in such applications, the size of the asperity contacts tends to decrease into the nano scale regime. Also with the increase in surface area to volume ratio in such systems, the surface force or adhesion becomes more prominent in contributing to surface interaction effects. Since the friction force depends on the real area of contact, which is strongly influenced by the presence of surface forces and surface roughness, it is important to analyze the effect of adhesion and roughness on the frictional behavior of small scale sliding systems. In the present study, the Hurtado and Kim model for the behavior of the friction stress is incorporated into the multi-asperity adhesive contact model of Roy Chowdhury and Ghosh which includes the asperity adhesion forces using the Johnson-Kendall-Roberts adhesion model. The well-established elastic adhesion index along with the plasticity index is used to consider the different conditions that arise as a result of varying load, material parameters and contact size. Results are obtained as the variation of coefficient of friction versus normal load for different combinations of the controlling parameters. It is found that the nano-scale effect in multi-asperity contacts is dominant for low values of adhesion index, small normal load and elastic contact conditions.

Keywords

Adhesive Friction, Roughness, Scale Effect

Received: August 24, 2015 / Accepted: September 20, 2015 / Published online: October 16, 2015

1. Introduction

Despite the huge progress in modelling engineering systems and processes, frictional phenomena continue to pose modelling problems. This highly unsatisfactory state of affairs has in the recent several decades been addressed by large number of groups covering fundamental areas of physics, mathematics and engineering. Since frictional forces arise as a result of interactions of surfaces in contact, it appears necessary to account for their complex topography. This clearly calls for a stochastic description of interactions and some averaging process by which a total response may be calculated. Macroscopic properties cannot be applied in situations where the size of contacting asperities is in the order of nanometers. Only detailed studies of friction at a single-asperity contact, under well-defined conditions and with nanometer-scale or even atomic-scale resolution, can result in an understanding of friction at fundamental level.

In the absence of adhesion, the Hertz [1] model has been shown to accurately describe the contact area between elastic spheres [2]. However, at small scales surface force is significant and must be included in any description of contact behavior. Johnson et al [3] concluded that Hertz theory is no longer applicable when surface forces at the contact are taken into account and also the force required to separate the bodies is independent of both the applied load and the elastic constants of the materials. The junctions responsible for the adhesion are also responsible for the frictional force. The idea that the friction is associated with adhesion is an old one, generally attributed to Desaguliers in the early years of the

* Corresponding author
E-mail address: psjume@gmail.com

eighteenth century, but it was Bowden & Tabor who made it a leading concept in their 'plastic junction' theory of friction. Adhesion is difficult to measure since elastic relaxation of the higher asperities, when the load is removed, breaks the adhesive contact of the lower junctions. To avoid these difficulties attempts are made to experiment with a single asperity contact, usually modeled by a spherical tip in contact with plane surface, in which real and apparent areas of contact coincide. This quest has been significantly advanced in recent years by the development of two novel instruments (i) the surface force apparatus (SFA) and (ii) the atomic force microscope (AFM). One of the fundamental postulates of friction is that at the microscopic or molecular level, the real area of contact is proportional to the load applied over the macroscopic or apparent area. Early experiments by Leonardo da Vinci, Amonton, Newton and many others [4] found that the friction force '*F*' needed to slide a mass across a surface varied in direct proportion to the weight of the object or the externally applied load '*P*' pressing down on it, but not to the area of contact between the moving surfaces. This is encapsulated in two of Amontons' laws of friction where the ratio of '*F*' to '*P*' defines the coefficient of friction as

$$\mu = \mathrm{F/P} \tag{1}$$

While we now know that the Eq. (1) is not exact when studied over large ranges of loads, contact areas, sliding velocities and adhering surfaces, it remains surprisingly good at describing the majority of rubbing surfaces involving both dry and lubricated, and especially not-adhering surfaces and the friction coefficient remains the most useful parameter for describing friction. Almost all the theories of friction, however, are highly model-dependent, and it is doubtful that they could account for all the parametric variations. Thus it is now well recognized that friction coefficient values depend on many factors such as surface roughness, surface energy, contact load and time [5] besides the contacting material pairs. In the present study, an attempt is made to consider the effect of surface roughness and surface energy on adhesive friction of small scale sliding rough surfaces using a scale-dependent model of friction.

2. Adhesive Contact and Friction

The well-known solution for the contact area between two elastic spheres was developed in the late nineteenth century by Hertz. The interference, contact radius, and maximum contact pressure are given by simple equations [2] which depend upon the Young's moduli, the Poisson's ratios, the radii of curvature, and the applied force. Various statistical models of multi-asperity contact have since been developed in order to determine the normal contact force, many of which are related in some way or other to the pioneering work of Greenwood and Williamson (GW) [6]. The adhesion model by Johnson, Kendall and Roberts (JKR)[3] assumes that the attractive intermolecular surface forces cause elastic deformation beyond that predicted by the Hertz theory, and produces a subsequent increase of the contact area. This model also assumes that the attractive forces are confined to the contact area and are zero outside the contact area. The other competing adhesion model by Derjaguin, Muller and Toporov (DMT) [7], on the other hand, assumes that the contact displacement and stress profiles remain the same as in the Hertz theory. However, these quantities are calculated for a higher effective load which includes the applied normal force as well as the attractive adhesive stresses acting outside of the contact area. Due to the assumptions involved, the JKR/DMT models are most suitable when the range of surface forces is small / large compared to the elastic deformations, as pointed out by Tabor [8]. Another adhesion model, introduced by Maugis[9], describes a continuous transition between the JKR and DMT models.

Chang, Etsion and Bogy (CEB) [10, 11] developed an elastic-plastic multi-asperity contact model for normal loading and friction based on volume conservation of a plastically deformed asperity control volume. Though some of their results are contrary to ordinary Amonton-Coulomb friction, but consistent with the results of various experimental investigations. Fuller and Tabor [12] investigated the effect of roughness on the adhesion between elastic bodies. A key parameter was identified which depends on surface energy, composite elastic modulus, standard deviation of asperity heights, and asperity curvature and governs the contact behavior. Roy Chowdhury and Ghosh (RG model) [13] investigated adhesive contact of friction using well known JKR model of adhesion and found that at low loads and high adhesion conditions the coefficient of friction is very high, load-dependent and reaches a constant value beyond a critical load which again depends on material parameters. A multi-asperity contact model based on Dugdale approximation [9] was presented by Maugis [14]. Although the friction force was not determined, it was speculated that the increase in contact force due to adhesion would result in increased friction.

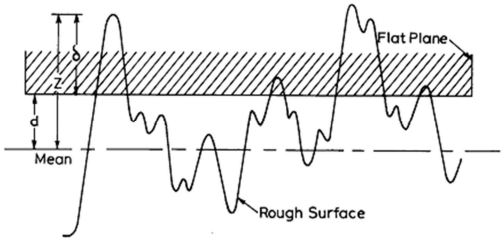

Fig 1. Contact between a rough deformable surface and a rigid flat plane.

Recent experimental evidences [15, 16] show that there is a significant change in the friction stress acting on a single asperity contact, as the contact area changes from the micro to nano scale. The scale dependence of the friction stress has recently been investigated by Hurtado and Kim (HK) [17, 18]. They presented a micromechanical dislocation model of frictional slip between two asperities for a wide range of contact radii. The HK model provides an expression for the behavior of the friction stress over a wide range of contact areas, including nano scale contacts.

In this paper, the frictional slip model of Hurtado and Kim and the adhesion contact model of RG [13] are combined in order to derive the relationship between the friction force '*F*' and the normal load '*P*'between two rough surfaces during a slip process with due consideration to the effect of surface forces and surface roughness for small scale sliding systems.

2.1. Loading Analysis

The contact of two rough surfaces is modeled as an equivalent single rough surface in contact with a rigid smooth surface as shown in Fig. 1. An adhesive contact such as the present one may be described in terms of elastic adhesion index $\theta = K\sigma^{3/2}R^{1/2}/\gamma R$ and plasticity index, $\psi = (E^*/H)(\sigma/R)^{1/2}$. Here σ is the standard deviation of asperity heights, $K = (4/3)E^*$, E* being the composite elastic moduli, *R* is the asperity radius, *H* is the hardness of the softer material and γ the work of adhesion. This elastic adhesion index is merely the ratio of the elastic force needed to push a sphere of radius *R* to a depth σ into an elastic solid of equivalent modulus of elasticity *E* to the adhesive force experienced by the sphere and ψ indicates the nature of contact. Following Roy Chowdhury and Ghosh [13] the contact load may be non-dimensionally written in terms of adhesion indices θ and ψ as

$$\overline{P}_l = \int_{\Delta_0}^{\Delta_{c1}} \left(\Delta^{3/2} - \frac{4.34}{\theta^{1/2}} \Delta^{3/4} \right) \varphi(\Delta) d\Delta + \int_{\Delta_{c1}}^{\infty} \left(\frac{4.745}{\psi} \Delta - \frac{6.28}{\theta} \right) \varphi(\Delta) d\Delta \tag{2}$$

where $\phi(\Delta)$ is the normalized asperity height distribution function in terms of normalized asperity deformation(Δ), $\overline{P}_l = P_l / KNR^{1/2}\sigma^{3/2}$, $h = d/\sigma$, $\Delta = \delta/\sigma$, $\Delta_c = \delta_c/\sigma$, $\Delta_{c1} = \delta_{c1}/\sigma$. Here d is the mean separation between surfaces and N is the number of asperities per unit area. In equation (2), Δ_0 and Δ_{c1} are the non-dimensional apparent displacements and Δ_c is the non-dimensional real displacement to be obtained from the following relations [13]

$$\Delta_{c1}^{3/4} - \frac{8.65}{\psi}\Delta_{c1}^{1/4} - \frac{4.34}{\theta^{1/2}} = 0 \tag{3}$$

$$\Delta_0 = 4.125/\theta^{2/3} \tag{4}$$

and

$$\Delta_c = \Delta_{c1} - \frac{2.89}{\theta^{1/2}}\Delta_{c1}^{1/4} \tag{5}$$

Traditionally, the Gaussian distribution is used to model the asperity heights and is given in normalized form by

$$\phi(\Delta) = 1/\sqrt{2\pi}\,\exp\left\{-(h+\Delta)^2/2\right\} \tag{6}$$

2.2. Friction Analysis

Recently Hurtado and Kim (HK model) [17, 18] presented a more accurate micromechanical dislocation model of friction between two asperities. It clearly establishes the friction stress as a varying function of contact size.The same is presented in Fig. 2 and it has three regions with two transitions. In the first region for very small contact sizes of less than 10nm, the slip is the result of the collective movement of atoms and it is called as concurrent slip, without mechanism of mobile dislocation and also it is independent of size leading to a constant value of τ_f. Then first transition takes place, i.e., in the second region, called as single dislocation assisted slip (SDA), which has a slope, depends upon the contact radius for about 10nm to 10 μm. In this region, it is a dislocation-nucleation-controlled friction process. Then second transition takes place, called as multiple dislocation cooperated (MDC) slip. It is dislocation mobility controlled process. It occurs at the contact size at which a nucleated dislocation stabilizes within the contact region. It is in line with the experiments conducted in AFM and SFA [15, 16]. According to their model for contact radii smaller than a critical value, in the concurrent slip region, the friction stress is constant. In the second region of SDA slip, the friction stress decreases as the contact radius increases until it reaches the third region, MDC slip, and there it becomes again independent of size.

The relationship between the non-dimensional friction stress and non-dimensional contact radius is given in the Fig. 2. The contact radius (*a*) is normalized ($\bar{a} = a/b$) by the Burgers vector (*b*) and the friction stress is normalized ($\bar{\tau}_f = \tau_f / G^*$) by the effective shear modulus given by $G^* = 2G_1G_2/(G_1+G_2)$ where G_1 and G_2 are the shear moduli of the contacting bodies. So, the dimensionless shear stress is a function of the contact radius and it can be approximated as [19]

$$\log(\bar{\tau}_{f1}) = \begin{cases} \log \bar{\tau}_{f1} & \bar{a} < \bar{a}_1 \\ M \log \bar{a} + B, & \bar{a}_1 < \bar{a} < \bar{a}_2 \\ \log \bar{\tau}_{f2} & \bar{a} > \bar{a}_2 \end{cases} \quad (7)$$

where the left and right limits of region-2 are $(\bar{a}_1, \bar{\tau}_{f1})$ and $(\bar{a}_2, \bar{\tau}_{f2})$ respectively. The constants of Eq. (7) are given by[19]

$$M = -\log(\bar{\tau}_{f1} / \bar{\tau}_{f2}) / \log(\bar{a}_2 / \bar{a}_1)$$

$$B = (\log(\bar{\tau}_{f1}) \log(\bar{a}_2) - \log(\bar{\tau}_{f2}) \log(\bar{a}_1)) / \log(\bar{a}_2 / \bar{a}_1)$$

where, M and B are, respectively, the slope and y-intercept of the line in region-2 of the log-log plot of the above Fig. 2. The friction force acting on a single asperity can be determined from the above equation by using the relationship $F_f = \pi a^2 \tau_f$. The total shear force F acting on the nominal contact area for a multi-asperity contact can be calculated integrating the shear forces acting on each asperity against the probability density function.

$$F = N \int_h^\infty F_f \phi(\Delta) d\Delta \quad (8)$$

In non-dimensional form, the friction force per unit area, may be obtained using Eq. (13) and (14) and is written as

$$\bar{F} = \frac{3(1-\upsilon)}{8\alpha\beta^2}[2\pi\bar{\tau}_{f1}\int_0^{\bar{a}_1} \bar{a}^2 \varphi(\Delta) d\Delta + 2\pi 10^B \int_{\bar{a}_1}^{\bar{a}_2} \bar{a}^{-M+2} \varphi(\Delta) d\Delta + 2\pi\bar{\tau}_{f2}\int_{\bar{a}_2}^{\infty} \bar{a}^2 \varphi(\Delta) d\Delta] \quad (9)$$

where, $\bar{F} = \frac{F}{KNR^{1/2}\sigma^{3/2}}$, $\alpha = (\sigma / R)^{1/2}$, $\beta = (\sigma R)^{1/2} / b$,

υ = Poisson's ratio,

$\bar{\tau}_{f1} = 1/43, \bar{\tau}_{f2} = \bar{\tau}_{f1} / 30, \bar{a}_1 = 28, \bar{a}_2 = 8\times10^4$.

The coefficient of friction is then calculated as

$$\mu = \bar{F} / \bar{P} \quad (10)$$

It may be noted here that for evaluating the friction force using eqn. (9), the non-dimensional contact radius ($\bar{a}$) needs to be expressed as function of the non-dimensional asperity deformation (Δ). The relation between $\bar{a}$ and Δ depends on the nature of contact, whether elastic or plastic.

For an elastic contact, i.e., for $\Delta < \Delta_c$,

$$\bar{a} = \frac{(R\delta)^{1/2}}{b} = \beta\Delta^{1/2} \quad (11)$$

For a plastic contact, i.e., for $\Delta \geq \Delta_c$,

$$\bar{a} = \frac{(2R\delta)^{1/2}}{b} = \sqrt{2}\beta\Delta^{1/2} \quad (12)$$

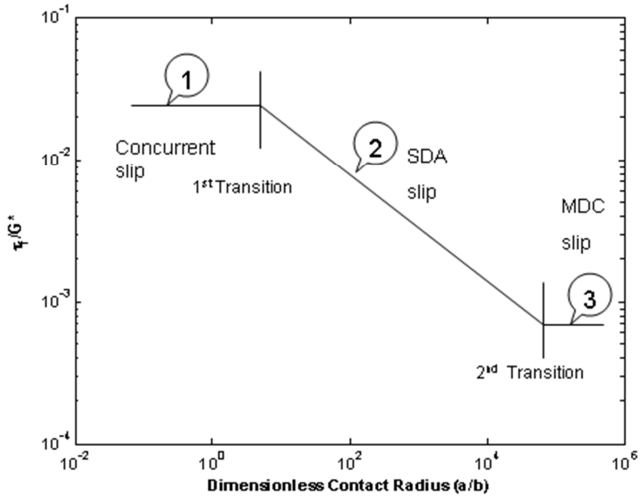

Fig 2. Relationship between the dimensionless friction stress and the dimensionless contact radius according to the HK model.

3. Results and Discussion

Equations established abovewere evaluated numerically and proper integral limits were set for equation (9) to check whether the dimensionless contact radius falls on elastic or plastic regime. The effect of adhesion on the coefficient of friction was investigated for typical combinations of θ and ψ for a constant practical value of α =0.01 and β =1000. Limiting values of θ is about 10, beyond which the effect of adhesion becomes insignificant due to the surface roughness effect. Thus the values of θ were selected between 2 to 25. The value of ψ, which indicates the nature of contact, is chosen as 0.5,0.9 and 2.5 so that the investigation covers the whole contact regime from fully elastic through elastic-plastic to fully plastic regimes. For ψ <0.6, the contact is predominantly elastic and for ψ >1.0, the contact is predominantly plastic.

Figs. 3-5 show the plot of non-dimensional load against non-dimensional mean separation, for different values of θ and ψ, which spread over from low to very high adhesion and elastic to plastic contact situations. The non-dimensional mean separation is considered to be between -1 and +2. Because at larger separations the chances of getting in contact will be very less and it shows almost zero load for higher positive mean separations. On the other hand, for very small separations the bulk deformations start and this asperity based model cannot be applied. In general, the contact load increases with decreasing mean separation. As the mean separation

decreases, the number of asperities coming into contact is more and needs more loading force to maintain a contact.

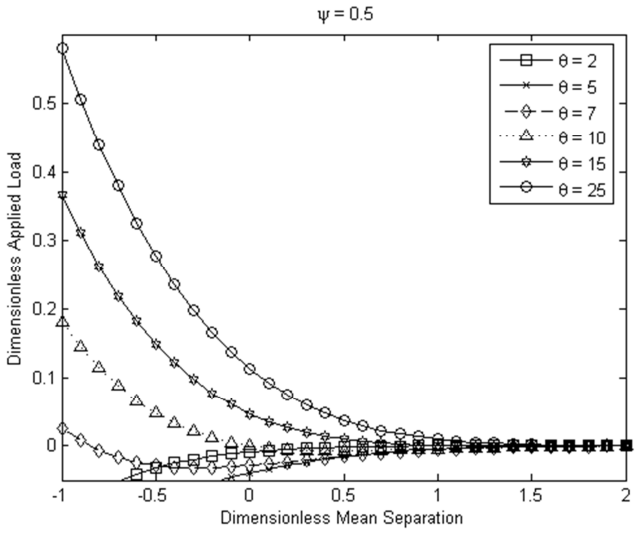

Fig 3. Plots of non dimensional loading force against non dimensional mean separation for different combinations of elastic adhesion index and at ψ =0.5.

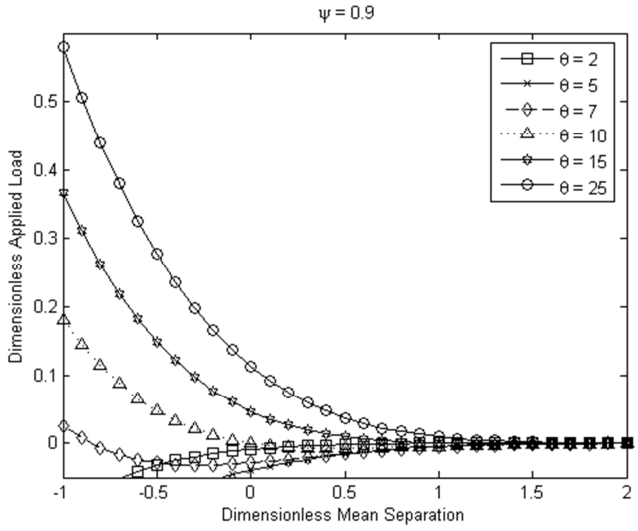

Fig 4. Plots of non dimensional loading force against non dimensional mean separation for different combinations of elastic adhesion index and at ψ =0.9.

In Fig. 3, it is observed that for low values of θ (θ=2 and 5) that correspond to high adhesion and at lower negative mean separation the loading forces are negative indicating tensile force. It shows that tensile load is required to maintain a particular mean separation due to high adhesion. However, at a particular mean separation below zero, the loading force is higher for a higher elastic adhesion index. High θ means low adhesion in elastically deformed asperities and hence a greater external load needs to be applied to maintain a contact. The same behavior is noted in higher values of ψ as shown in Figs.4 and 5. But the loading force is more for high plasticity index. High value of ψ corresponds to low adhesion regime or the contacts are fully in plastic regime, which needs larger amount of load to attain this state. It may be noted that when ψ is 0.9, i.e., in elastic plastic regime the variation compared to fully elastic regime is negligible.

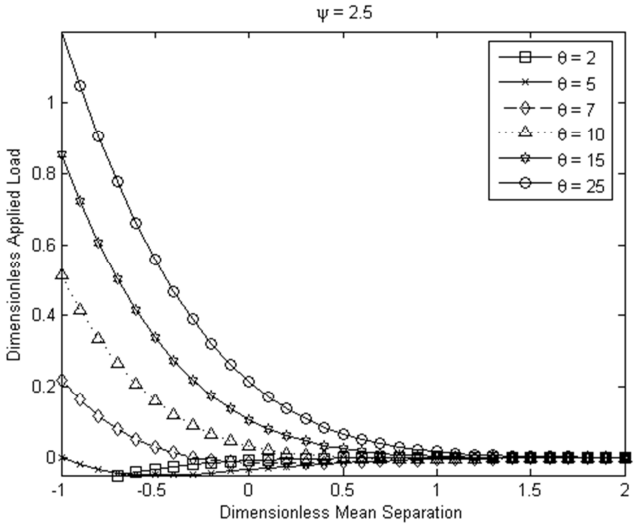

Fig 5. Plots of non-dimensional loading force against non-dimensional mean separation for different combinations of elastic adhesion index and at ψ =2.5.

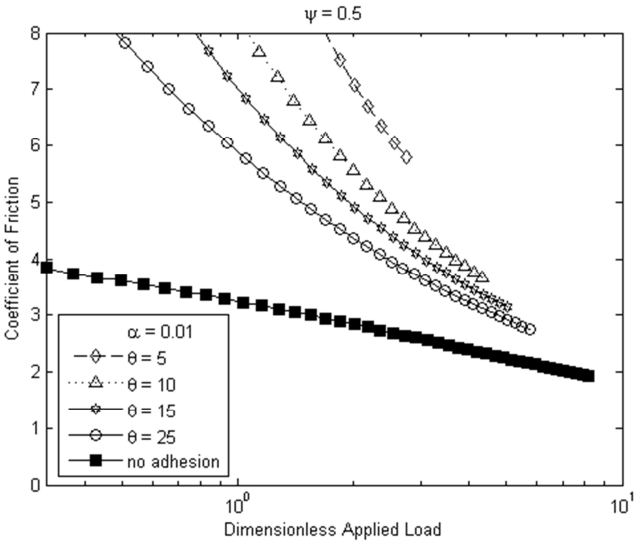

Fig 6. Plots of coefficient of friction against non-dimensional loading force at ψ =0.5.

Figs.6-8 show the plot of coefficient of friction μ against the normal load for different values of θ and ψ. In general it is found that friction is highly load dependent. At low normal load it predicts very high friction because of the high adhesional effect. For a particular low normal load, the coefficient of friction is more when θ is low that indicates high adhesion case. At relatively higher θ, μ is low. Progressive increase in load results in decrease in μ values and the curves tend to merge at relatively higher normal loads leading to a constant value of the coefficient of friction. This is more evident in the case of higher value of ψ. Lower normal

loads indicate that, the number of asperities in contact is very less and it may be assumed as a micro or nano contact situation in which the friction stress is greatest and the effect of adhesion induced friction is dominant. To compare with the adhesion effect the no-adhesion contact condition is also considered in these figures. For no-adhesion case, load-dependency of friction is present but to a very small extent as evidenced from these plots. It may be noted here that the effect of adhesion on friction coefficient is very prominent for low load regimes. It is also seen from these plots that for a particular normal load and mean separation, the value of μ is relatively high in the case of elastic regime compared to plastic regime.

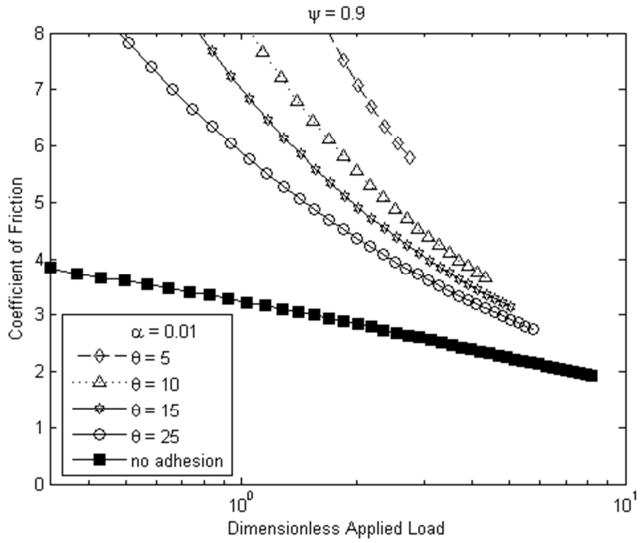

Fig 7. Plots of coefficient of friction against non-dimensional loading force at ψ =0.9.

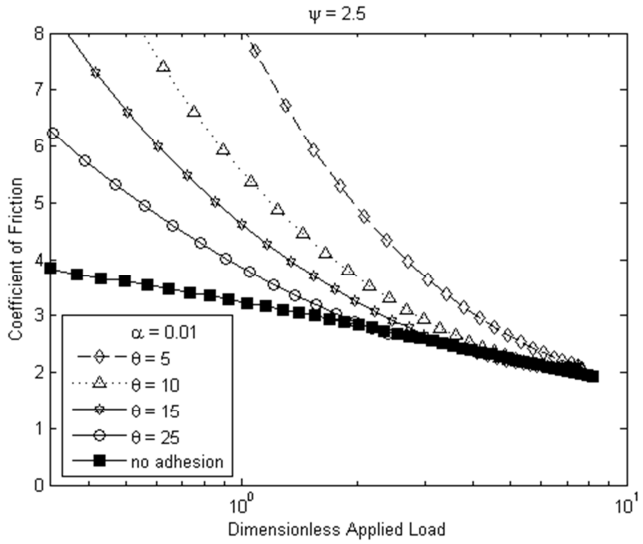

Fig 8. Plots of coefficient of friction against non-dimensional loading force at ψ =2.5.

In majority of models, the three-point peak (asperity) of the GW model has formed the basis of analysis. But recently, in spite of the wide acceptance and popularity, adequacy of the GW model has been questioned by none other than Greenwood [20] himself. According to him his original idea of three point peaks is incorrect as an asperity cannot be defined only as a point higher than its two immediate neighbors. The GW model has been found in good qualitative agreement with experiments, but all attempts to obtain quantitative agreement face the difficulty of obtaining unique values of summit density and curvature. It is well known that height-dependent parameters depend slightly on the longest wavelength measured, whereas parameters such as slopes and curvatures depend strongly on the shortest wavelength measured. It one tries to consider all the wavelengths of real profiles, all texture-dependent roughness parameters will tend to infinity and the conclusion is inevitable "3-point peaks are just an artifact of the profile, not real physical features". Therefore, the approximation of asperities in terms of peaks or summits is problematic and in an engineering problem, an asperity should be related to a contact. This paved the way for introduction of a new multiple-point asperity model called the n-point asperity model, put forward by Hariri et al [21].The n-point asperity model developed by Hariri et al. [21] defines the rough surface in more realistic way as compared to other available techniques. So use of this model is expected to yield comparatively more accurate results of analysis. Based on this new n-point asperity model, the rough surface contact problems for various contact conditions have been considered earlier [22-27]. Future studies will consider the present analysis using n-point asperity model.

4. Conclusion

In this paper the single asperity scale-dependent friction model of Hurtado and Kim has been incorporated into a multi-asperity model for contact which includes the effect of asperity adhesion using Roy Chowdhury and Ghosh model. The well-established elastic adhesion indices along with the plasticity index are used to consider the different conditions that arise as a result of varying load, material parameters and contact size. Results are obtained as the variation of coefficient of friction versus normal load for different combinations of the controlling parameters. It is found that the nano-scale effect in multi-asperity contacts is dominant for low values of adhesion indices, small normal load and elastic contact situations.

Nomenclature

Symbol	Meaning	Unit
B	y-intercept of line in region-2 of the	-

	Hurtado and Kim model	
E^*	Composite elastic modulus	(N/m^2)
F	Friction force	(N)
F_f	Friction force on a single asperity	(N)
$\overline{F}$	Dimensionless friction force	-
G	Shear modulus	(N/m^2)
G^*	Effective shear modulus	(N/m^2)
K	4/3E*	(N/m^2)
M	Slope of line in region -2 of the Hurtado and Kim model	-
N	Number of asperities	-
P	Normal force	(N)
P_l	total loading force	(N)
$\overline{P}_l$	Dimensionless normal force	-
R	Asperity radius	(m)
a	Contact radius	(m)
$\overline{a}$	Dimensionless contact radius	-
b	Burgers vector magnitude	(nm)
d	Separation distance of surfaces relative to the mean of asperity heights	(m)
h	d/σ	-
z	Asperity height with respect to mean of asperity heights	(m)
α	Surface roughness parameter	-
θ	Elastic adhesion index	-
γ	Work of adhesion	(m^{-2})
ψ	Plasticity index	-
ϕ	Asperity peak probability distribution	
δ	asperity deformation	(m)
δ_1	apparent displacement of an asperity	(m)
δ_c	critical displacement of an asperity for yielding inception	(m)
δ_{c1}	Apparent critical displacement of an asperity for yielding inception	(m)
μ	Static coefficient of friction	-
σ	Standard deviation of asperity peak heights	(m)
τ_f	Friction stress	(N/m^2)
$\overline{\tau}_f$	Dimensionless friction stress	-
τ_{f1}, τ_{f2}	Shear stress at upper and lower limits of the HK model	(N/m^2)

References

[1] Hertz, H.J., 1881, ReineAngew. Math., 92:156.

[2] Johnson, K.L., 1985, *Contact Mechanics*, Univ. Press, Cambridge.

[3] Johnson, K. L., Kendall, K., and Roberts, A. D., 1971, "Surface Energy and the Contact of Elastic Solids," Proc. R. Soc. London, A324: 301– 313.

[4] Dowson, D., 1979, *History of Tribology*, Longman, London.

[5] Chang, W.R., Etsion, I., and D. B. Bogy, 1988, "Adhesion Model for Metallic Rough Surfaces", Trans. ASME, J. Tribology, 110: 50-56.

[6] Greenwood, J. A., and Williamson, J. B. P., 1966, "Contact of Nominally Flat Surfaces," Proc. R. Soc. London, A295: 300–319.

[7] Derjaguin, B. V., Muller, V. M., and Toporov, Y. P., 1975, "Effect of Contact Deformations on the Adhesion of Particles," J. Colloid Interface Sci.,53: 314–326.

[8] Tabor, D., 1976, "Surface Forces and Surface Interactions," J. Colloid Interface Sci., 58: 2–13.

[9] Maugis, D., 1992, "Adhesion of Spheres: The JKR-DMT Transition Using a Dugdale Model," J. Colloid Interface Sci., 150: 243–269.

[10] Chang, R. W., Etsion, I., and Bogy, D. B., 1987, "An Elastic-Plastic Model for the Contact of Rough Surfaces," ASME J. Tribol.,109: 257–263.

[11] Chang, W. R., Etsion, I. and Bogy, D. B., 1988, "Static Friction Coefficient Model for Metallic Rough Surfaces". Trans. ASME, J. Tribology, 110: 57-63.

[12] Fuller, K. N. G., and Tabor, D., 1975, "The Effect of Surface Roughness on the Adhesion of Elastic Solids," Proc. R. Soc. London, A345: 327– 342.

[13] Roy Chowdhury, S. K. and Ghosh, P., 1994, "Adhesion and Adhesional Friction at the Contact between Solids". Wear, 174: 9-19.

[14] Maugis, D., 1996, "On the Contact and Adhesion of Rough Surfaces," J. Adhes. Sci. Technol., 10: 161–175.

[15] Carpick, R. W., Agrait, N., Ogletree, D. F. and Salmeron, M., 1996, "Measurement of Interfacial Shear (friction) with an Ultrahigh Vacuum Atomic Force Microscope". J. Vac. Sci. Technol. B, 14: 1289-1295.

[16] Homola, A. M., Israelachvili, J. N., McGuiggan, P. M. and Gee, M. L., 1990, "Fundamental Experimental studies in Tribology: the Transition from 'Interfacial' Friction of Undamaged Molecularly Smooth Surfaces to 'Normal' Friction with wear". Wear, 136: 65-83.

[17] Hurtado, J. A., and Kim, K.-S., 1999, "Scale Effects in Friction of Single Asperity Contacts: Part I; From Concurrent Slip to Single-Dislocation-Assisted Slip," Proc. R. Soc. London, A455: 3363–3384.

[18] Hurtado, J. A., and Kim, K.-S., 1999, ‘‘Scale Effects in Friction in Single Asperity Contacts: Part II; Multiple-Dislocation-Cooperated Slip,’’ Proc. R. Soc. London, A455: 3385–3400.

[19] Adams, G. G., Muftu, S. and MohdAzhar, N., 2003, “A Scale-Dependent Model for Multi-Asperity Contact and Friction”, Trans. ASME: J. Tribology, 125: 700-708.

[20] Greenwood, J. A. and Wu, J. J., 2001,“Surface roughness and contact: An apology”, Meccanica, 36: 617–630.

[21] Hariri, A., Zu, J. W. and Ben Mrad, R. 2006, “n-Point asperity model for contact between nominally flat surfaces,” Trans. ASME J. Tribol. 128: 505-514.

[22] Hariri, A., Zu. J. W.,& Ben Mrad. R., 2006, “Modeling of Elastic/Plastic Contact between Nominally Flat Rough Surfaces Using an n-Point Asperity Model”, ASME Journal of Tribology, 128, 876-885.

[23] Sahoo, P., Mitra, A., &Saha, K. 2009, “Elastic - Plastic Adhesive Contact of Rough Surfaces using n-Point Asperity Model”, Journal of Physics. D, Applied Physics, 42(6), 1–13.

[24] Waghmare, A. K., &Sahoo, P. 2014,“A Study of Elastic-Plastic Contact of Rough Surfaces using n-point asperity model”, Procedia Material Science, 5, 1716–1725.

[25] Waghmare, A. K., &Sahoo, P., 2014, “Elastic-plastic Adhesive Contact of Rough Surfaces Based on Accurate FEA study Using n-Point Asperity Model,” International Journal of Surface Engineering and Interdisciplinary Material Science, 2(2), 1-22.

[26] Waghmare, A. K., &Sahoo, P. 2015, “Adhesive Friction at the Contact between Rough Surfaces using n-Point Asperity Model,” Engineering Science and Technology, an International Journal, 18, 463-474.

[27] Waghmare, A. K., &Sahoo, P., 2015, “Adhesive Wear at the Contact between Rough Surfaces using n-Point Asperity Model,” Proc. International Conference on Computing in Mechanical Engineering-2015. (in press).